ISPARTA UYGULAMALI BİLİMLER ÜNİVERSİTESİ

Turkish Journal of Forestry | Türkiye Ormancılık Dergisi
2025, 26(1): 25-35 | Research article (Araştırma makalesi)

Generation of digital terrain models using different geospatial measurement technologies: A comparative analysis of the terrain data sets

Ali Karaca[a], **Ender Buğday**[b,*]

Abstract: Since early civilizations, the growing need for information has driven continuous advancements in surveying and photogrammetry, particularly with modern technologies enhancing measurement techniques and the integration of global positioning systems across terrestrial, aerial, and satellite platforms. Since the early twenty-first century, technologies such as GPS, mobile phones, GNSS-CORS, and UAVs have rapidly become integral to practical measurements across various sectors, including construction, mining, aviation, agriculture, and forestry. In this study, topographic measurement devices with different measurement sensitivities, such as GPS, GNSS-CORS, mobile phones and UAVs, were measured in the same size area and compared in terms of measurement time, precision and mapping. In addition, digital elevation values were calculated for the same area and mapped in the Google Earth software environment from satellite data, a widely referenced remote sensing dataset. These different measurement data obtained were compared on the same plane and as a result, it was determined that GNSS-CORS and RTK-UAV devices with RTK provided high precision data, followed by UAV without RTK device, Google Earth data set, mobile phone and GPS device. Upon examination of the results of this study, it was determined that UAV technology is particularly compatible with research endeavors demanding high precision and rapid data acquisition. Conversely, for studies where high sensitivity is not a primary consideration, measurements derived from GPS and mobile phone data may offer a suitable alternative.
Keywords: Unmanned aerial vehicle, GNSS-CORS, GPS, Terrain measurement

Farklı coğrafi ölçüm teknolojilerini kullanarak sayısal arazi modellerinin üretilmesi: Arazi veri setlerinin karşılaştırmalı analizi

Öz: Eski medeniyetlerden bu yana, artan bilgi ihtiyacı, özellikle ölçüm tekniklerini ve küresel konumlandırma sistemlerinin karasal, hava ve uydu platformları arasında entegrasyonunu geliştiren modern teknolojilerle birlikte, arazi ölçümü ve fotogrametri alanında sürekli ilerlemelere yol açmıştır. Yirmi birinci yüzyılın başlarından bu yana, GPS, cep telefonları, GNSS-CORS ve İHA'lar gibi teknolojiler, inşaat, madencilik, havacılık, tarım ve ormancılık dahil olmak üzere çeşitli sektörlerde pratik ölçümlerin ayrılmaz bir parçası haline gelmiştir. Bu çalışmada, GPS, GNSS-CORS, cep telefonları ve İHA'lar gibi farklı ölçüm hassasiyetlerine sahip topoğrafik ölçüm cihazları aynı büyüklükteki alanda ölçülmüş ve ölçüm süresi, hassasiyet ve haritalama açısından karşılaştırılmıştır. Ayrıca, aynı alan için sayısal yükseklik değerleri hesaplanmış ve yaygın olarak referans alınan bir uzaktan algılama veri kümesi olan uydu verilerinden Google Earth yazılım ortamında haritalanmıştır. Elde edilen bu farklı ölçüm verileri aynı düzlemde karşılaştırılmış ve sonuç olarak RTK özellikli GNSS-CORS ve RTK-İHA cihazlarının yüksek hassasiyetli veri sağladığı, bunu RTK cihazı olmayan İHA, Google Earth veri seti, cep telefonu ve GPS cihazının izlediği belirlenmiştir. Çalışmada elde edilen sonuçlar incelendiğinde, yüksek hassasiyet ve kısa süreli ölçüm gerektiren çalışmalarda İHA kullanımının daha etkili olduğu, yüksek hassasiyet istenmeyen çalışmalarda ise GPS ve cep telefonu ile yapılan ölçümlerin kullanılabileceği sonucuna varılmıştır.
Anahtar kelimeler: İnsansız hava aracı, GNSS-CORS, GPS, Arazi ölçümü

1. Introduction

In response to the rapid surge in global population, there has been a concurrent escalation in demands across virtually every sector. As the world evolves at an unprecedented pace, there is an increasing imperative for more meticulous planning activities. In this regard, advancements in measurement technologies and devices within the engineering domain are progressing and improving gradually (Eryılmaz, 2019). The measurement techniques and instruments prevalent in engineering research are continually undergoing enhancements, with updated products being introduced to the market over time. Notable examples of measurement devices utilized within the engineering sector include the Global Positioning System (GPS) (Karaali and Yıldırım, 1996; Huggins et al., 2020), the Global Navigation Satellite Systems-Continuously Operating Reference Stations (GNSS-CORS) (Kahveci, 2009; Fan et al., 2024), total stations (Karagöz et al., 2020; Putra et al., 2023), and

[a] Governorship of Çankırı, Special Provincial Administration, Çankırı, Türkiye
[b] Çankırı Karatekin University, Faculty of Forestry, Department of Forest Engineering, Çankırı, Türkiye
[*] **Corresponding author** (İletişim yazarı): ebugday@karatekin.edu.tr
Received (Geliş tarihi): 17.08.2024, **Accepted** (Kabul tarihi): 22.01.2025

Citation (Atıf)**:** Karaca, A., Buğday, E., 2025. Generation of digital terrain models using different geospatial measurement technologies: A comparative analysis of the terrain data sets. Turkish Journal of Forestry, 26(1): 25-35.
DOI: 10.18182/tjf.1534998

Unmanned Aerial Vehicles (UAVs) (Buğday, 2019; Śledź et al., 2021).

As technology continues to advance, handheld GPS units, GNSS-CORS devices, and total stations have become widely used in land surveying research. Recently, UAVs have also been incorporated into this suite of tools. While the capabilities of these devices vary depending on the specific measurement objectives and required data accuracy, they remain effective within the constraints of their technical specifications and the desired measurement sensitivity (Bülbül et al., 2015). The operational boundaries of each device are explicitly defined by the manufacturers, based on their design parameters and performance characteristics. The operational limits of each measurement device are delineated by the manufacturers.

In the context of forested areas and their adjacent environments, it is well-documented that measurements are inherently challenging, necessitating considerable labor and time compared to measurements in flat terrains. Given that the majority of forested regions in Türkiye are situated on mountainous and sloping landscapes, measurement activities are generally perceived as arduous and protracted. The sensitivity and accuracy of measurement instruments employed in engineering studies are contingent upon the technological capabilities of the devices utilized. Beyond the complexities introduced by rugged terrain and adverse weather conditions, it is crucial to assess the performance of these instruments, evaluate their operational durations, and determine their efficiency and costs to enhance the effectiveness and rationality of measurement practices. Therefore, identifying the appropriate devices for specific applications and contexts, and elucidating their efficiency and cost implications, is of paramount importance.

UAVs have become indispensable across a wide range of sectors due to their reliability and practical utility. Their applications are notably prevalent in fields such as aviation (Grindley et al., 2024), energy (Boukoberine et al., 2019), security and emergency response (Robakowska et al., 2022), logistics (Gupta et al., 2021), mining (Şanlıyüksel Yücel and Yücel, 2017) (Ren et al., 2019), construction (Martinez et al., 2020; Park et al., 2022), and environmental sciences (Fascista, 2022). In particular, the forestry sector has witnessed a significant integration of UAV technology, where these devices are employed for a multitude of specialized tasks. These include detailed land analysis and mapping (Schiefer et al., 2020), precise excavation and fill calculations (Tercan, 2017; Buğday, 2018), comprehensive road project evaluations (Akgül et al., 2016; Julge et al., 2019), and the measurement of various parameters related to tree and stand characteristics (Durgun et al., 2022; Durgun et al., 2023). The deployment of UAVs in these activities not only enhances operational efficiency but also provides valuable data that supports informed decision-making and resource management within the forestry.

In this study, a land area of same size (1 hectare) was surveyed using GPS, mobile phone, GNSS-CORS, and UAVs, and a benefit/cost analysis was conducted based on various resolution levels. Currently, these technologies are extensively employed in land surveying as well as in calculations for excavation and earthmoving projects. Given that the forestry sector is an engineering discipline requiring such measurements and evaluations, these devices are periodically utilized within this field. In forestry terrain measurement studies, the selection of measurement tools is influenced by several factors, including the size of the area to be surveyed, the required measurement precision, the availability of trained personnel, the timeframe allocated for the measurement, and the budget constraints. It is essential to evaluate these factors within a benefit/cost framework, presenting numerical data to inform decision-making. In this context, various measurement devices with differing technical specifications were employed simultaneously at the same location, allowing for comparative analysis. Consequently, recommendations were made concerning the optimal tool for the area size, measurement duration, and cost considerations (both renting and purchasing).

2. Material and method

2.1. Study area

This study was carried out within the forest area border of Akbaş Village, a forest village located in Çerkeş district of Çankırı province. The study area is shown in Figure 1. The size of the study area was limited to 1 ha for the purpose of using unit calculations. Within the scope of this study, measurement times were calculated using Garmin Oregon 550 brand handheld GPS device, CHC-X91 brand GNSS-CORS device, DJI Phantom 4 and DJI Phantom 4 RTK UAV-drone devices and iPhone 13 Pro mobile phone. The location accuracies of these devices are Garmin 3-5 m., CHC-X91 device 1-2 cm., Phantom drone 4 1-2 m., Phantom 4 RTK drone (1-3 cm), and iPhone 13 Pro 5 meters.

In this study, devices characterized by different technological attributes and varying levels of measurement precision, all employing global positioning systems, were utilized. The devices in question included a handheld GPS unit (Garmin, 2024), a GNSS-CORS device (CHC, 2024), DJI Phantom 4 and DJI Phantom 4 RTK drones, as well as a mobile phone (Apple, 2024).

In this study, calculations were made considering the technical specifications and technological capabilities of all measurement devices used, and the results were presented in the results section by comparing the data of the Digital Elevation Model (DEM) and Digital Terrain Model (DTM) and by presenting them in tables and graphics. Within the scope of this study, Phantom 4 (DJI, 2024a) and Phantom 4 RTK (DJI, 2024b) devices, which are increasingly used in photogrammetric measurement studies, were preferred. Technical information about these devices is given in Table 1.

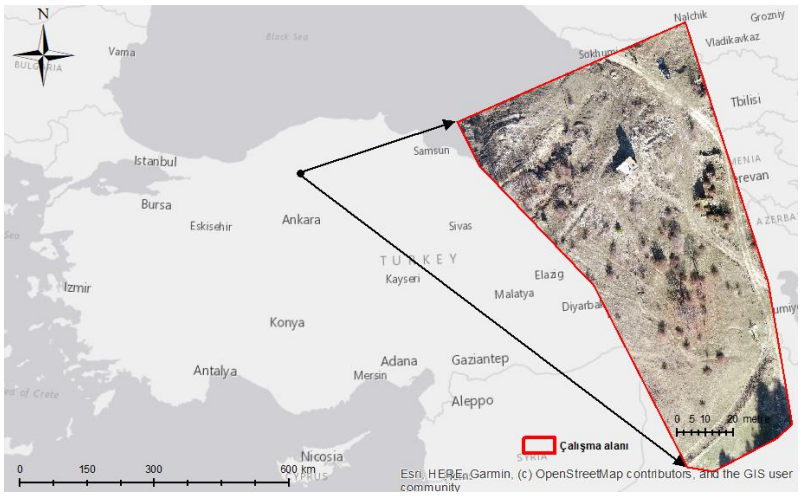

Figure 1. Location of the study area

2.2. Method

Measurements were conducted across the same geographic area using each of these devices. Additionally, satellite-derived height data from Google Earth was employed for comparative analysis. Specifically, GNSS-CORS, GPS, and mobile phone devices (utilizing GPS tracks software for terrestrial measurement) were employed to record data while traversing the area in parallel, with data points collected at five-meter intervals (Figure 2). Subsequently, the Phantom 4 and Phantom 4 RTK drones were operated autonomously to capture aerial imagery of the terrain. The resulting data are systematically presented in tabular and graphical formats within the results section.

The performance of all measuring devices in this study is evaluated using the Root Mean Square Error (RMSE), as described by Equation (1), a method commonly employed in the international literature (Famiglietti et al., 2021).

$$RMSE = \sqrt{[\sum_{i=1}^{n}(Pi - Oi)2 / n]} \quad (1)$$

In this equation, Pi: the estimated value for the i-th observation in the data set, Oi: the observed value for the i-th observation in the data set, and n: the number of samples. The Root Mean Square Error (RMSE) can range from zero to infinity. A model exhibiting an RMSE value close to zero indicates minimal error, signifying that the model's predictions are highly accurate. Specifically, an RMSE of zero denotes a complete absence of error (Famiglietti et al., 2021). Given that this study incorporates GIS-based data, the evaluation of spatial resolution and sensitivity also emerges as a crucial criterion. In this context, data exhibiting minimal error rates, and the highest precision were assessed concurrently. Consequently, datasets characterized by low error rates and reduced sensitivity were employed for optimization, whereas datasets with higher error rates and increased sensitivity were systematically catalogued and tabulated. Additionally, digital elevation data, frequently utilized in remote sensing, was obtained from the internet (www.usgs.gov) and restricted to the study area, with sensitivity values incorporated into the corresponding tables. The study further investigated the duration required to measure land data using various tools and assessed their sensitivity rates. Moreover, cost information was provided detailing the procurement expenses of the devices used in the study and the overall cost of the measurement activities, expressed in dollars. The cost calculation was conducted by considering only the purchasing costs, without taking into account any additional factors such as transportation, installation, maintenance, or operational expenses. The coordinate and altitude data collected from multiple devices deployed in the study area were evaluated for their accuracy, with the GNSS-CORS device serving as the reference standard for comparison. This evaluation aimed to assess the reliability and precision of the data obtained from each device in relation to the high-accuracy measurements provided by the GNSS-CORS system.

Table 1. Some technical specifications of the UAV devices

Specification	Phantom 4	Phantom 4 RTK
Takeoff weight	1380 g	1391 g
Battery	5870 mAH LiPo	6000 mAH LiPo
Camera sensor	1/2.3” CMOS, 4K	1" CMOS, 4K
Maximum speed	40 kmph-50 kmph	50 kmph-70 kmph
Flight distance	5000 m-6000 m	6500 m-7000 m
Maximum flight time	28 minutes	30 minutes

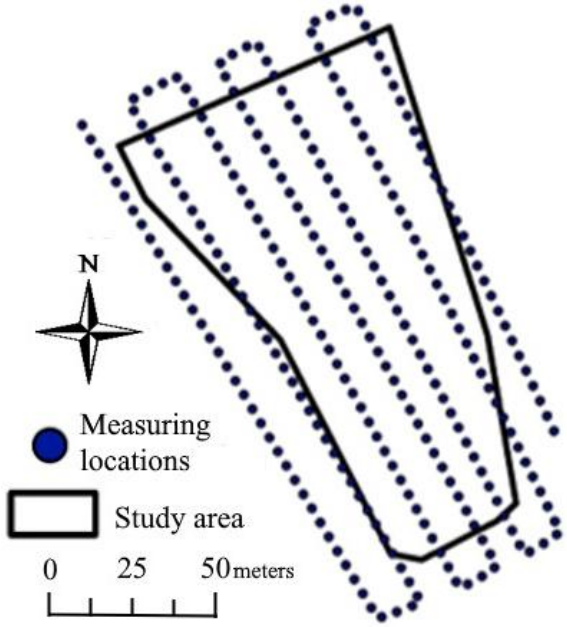

Figure 2. Study area measurement locations

2.3. Measurements using survey devices and their generation process of DEM data sets

In this study, devices including the CHC-X91 GNSS-CORS, the Garmin Oregon 550 handheld GPS, and the iPhone 13 Pro were employed. In the GPS devices used in this study, WGS84 UTM Projection Zone 36N was used as the geodetic reference system. Data points collected from these GPS, GNSS-CORS, and mobile phone devices within the study area were initially transferred to a computer system. Subsequently, the data obtained from the GNSS-CORS device were processed utilizing NetCAD GIS 8 software. In contrast, data from the GPS, mobile phone, and Google Earth sources were analyzed using ArcGIS 10.3 software. Individual DEMs were generated for each data source. The elevation data was employed to generate raster datasets of the measured terrain surfaces through the application of the "IDW" (Inverse Distance Weighting) (ESRI, 2023), interpolation method within the "Spatial Analysis – Interpolation" module of ArcGIS software.

2.4. Measurement and Data Generation Process for DTM data sets with UAV Devices

The UAV data is generated by transferring images from the UAV devices to a computer system, where they are processed using various photogrammetric software applications, such as Pix4D and Agisoft. For this study Pix4D, a widely utilized software in the field of photogrammetry, was selected. The images acquired from the study area are incorporated into the software after defining the coordinate system. To generate three-dimensional terrain data within the Pix4D interface, the 3D maps feature was employed to activate the point cloud data and the Raster DTM section was utilized to delineate the terrain surface. Following these procedures, the Ground Control Point (GCP) coordinates were input into the system (10 GCPs in total), initiating the surface creation process. In this study, Phantom 4 and Phantom 4 RTK drones were employed. Utilizing these devices, a flight (flying at 80 m above ground) was conducted over Akbaş village, ensuring coverage of the entire area. Prior to the UAV operations, the locations of the GCPs were delineated on the ground using spray paint, and their coordinates were accurately recorded with the assistance of a GNSS-CORS device (Figure 3). The flights were conducted at a speed of 11 km/h from a height of 80 m with 80% frontal and 70% side overlap.

The images captured during the aerial surveys conducted over the study area underwent calibration utilizing GCPs data to ensure spatial accuracy. Following this calibration process, the images were processed and converted into a detailed point cloud and a three-dimensional terrain model. This transformation was achieved through the superimposition of an orthomosaic onto the point cloud, leveraging the capabilities of Pix4D software to integrate and render the data comprehensively. The resulting models provide an accurate and visually coherent representation of the terrain, facilitating advanced analysis and interpretation. In this study, to ascertain and compare the latitude, longitude, and altitude values for identical locations across all generated land surfaces, random points were generated using the "Random Points" function (ESRI, 2022) within the ArcGIS software environment. The terrain surface models, specifically DEMs and DTMs, created for this study served as the foundational reference. Elevation values for these random points (total 100 points) were subsequently computed using ArcGIS 10.3. Following this calculation, the altitude values derived from all DEM and DTM datasets were consolidated into a single table. The GNSS-CORS measurement data were then subtracted from these values to determine the altitude discrepancies.

Figure 3. GCP marking and GNSS-CORS device measurement pictures on the study area

3. Results and discussion

3.1. Generation process results of DEM data sets obtained from GNSS-CORS, GPS, Mobile phone, Google Earth

The data acquired from the GNSS-CORS device was imported into the NetCAD GIS 8 software, where triangulation was executed utilizing elevation data derived from point measurements. In this process, the surface elevation data served as a reference, while unmeasured areas were interpolated and aligned accordingly. Subsequently, the elevation data was computed within the software environment. In the subsequent phase, contour lines with a 1-meter interval were generated based on the triangulated surface (Figure 4).

This data was utilized to construct a digital terrain model using elevation information derived from point measurements. The elevation data served as the reference for the terrain, with unmeasured terrain sections being interpolated and integrated within the software to accurately represent the terrain surface. Subsequently, the elevation data was employed to generate raster datasets of the measured terrain surfaces through the application of the IDW interpolation method within the "Spatial Analysis – Interpolation" module of ArcGIS (Figure 5).

In the context of this study, Figure 6 presents elevation raster data generated from DEMs that were derived using datasets obtained from GNSS-CORS, GPS technology, mobile phone measurements, and Google Earth platform within the study area. The results of minimum and maximum elevation data provided from DEM data were given Figure 7.

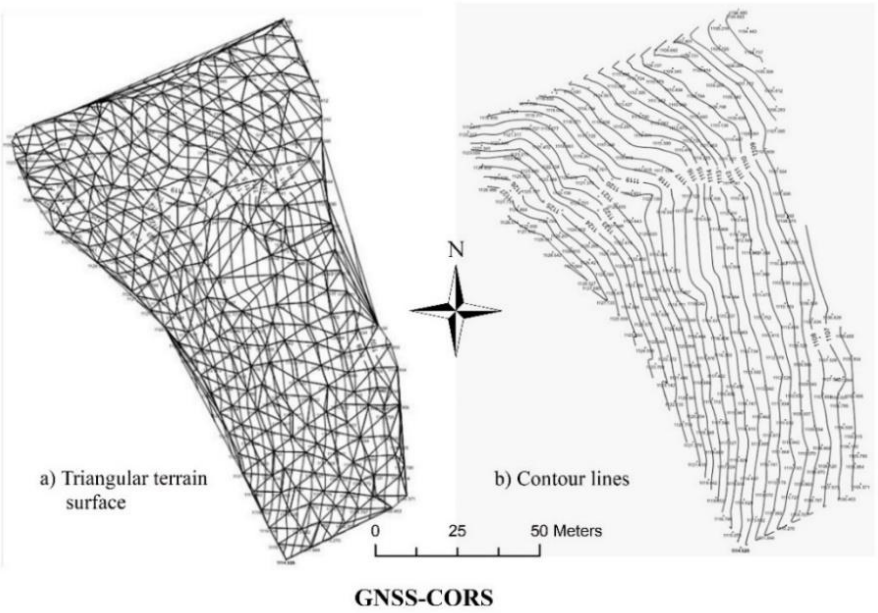

Figure 4. GNSS-CORS data: a) Triangular terrain surface, b) Contour lines

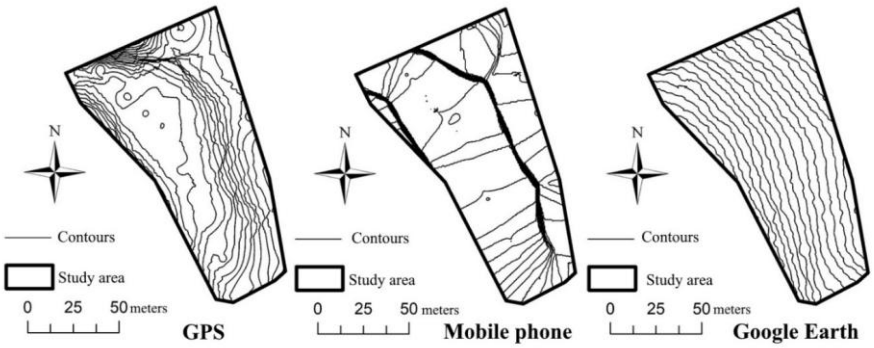

Figure 5. Contours obtained a) GPS b) Mobile phone and c) Google Earth

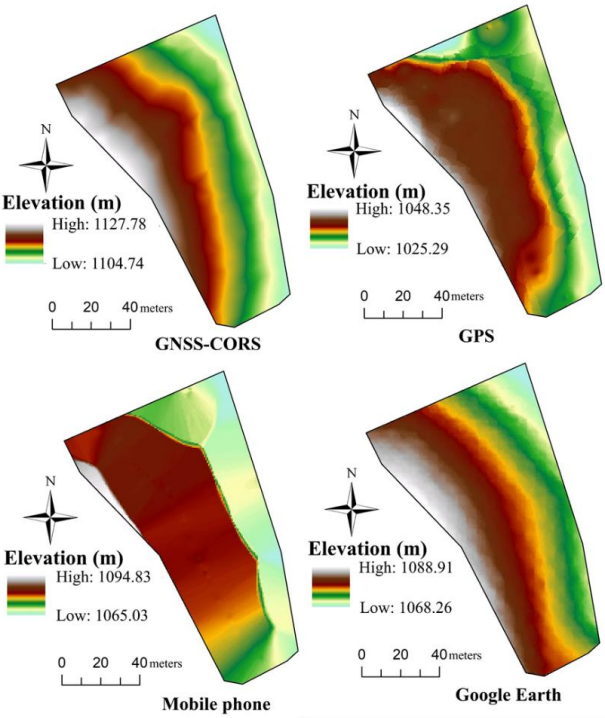

Figure 6. DEM data generated from GNSS-CORS, GPS, mobile phone devices and Google Earth

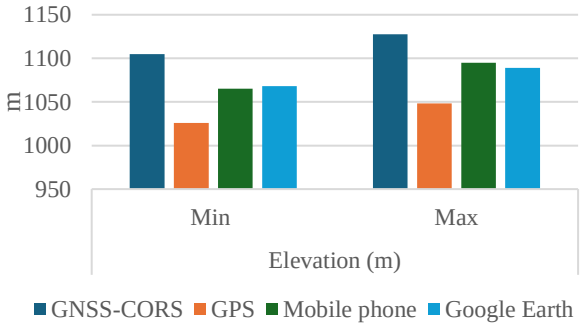

Figure 7. Elevations (m) of DEMs generated from GNSS-CORS, GPS, Mobile phone, Google Earth

The GNSS-CORS exhibits the highest minimum elevation at 1104.74 meters and the highest maximum elevation at 1127.78 meters, thereby encompassing an elevation range of 23.04 meters when the graph given in Figure 7 is examined. In contrast, the GPS device records the lowest minimum elevation at 1025.29 meters and the lowest maximum elevation at 1048.35 meters, resulting in an elevation range of 23.06 meters. The Mobile phone system provides the most extensive range, measuring 29.80 meters, with minimum and maximum elevations of 1065.03 meters and 1094.83 meters, respectively. Google Earth software displays the smallest range at 20.65 meters, with minimum and maximum elevations of 1068.26 meters and 1088.91 meters. In summary, the GNSS-CORS device provides the highest elevation values with a moderate range, while the GPS device records the lowest elevation value, exhibiting a range comparable to that of the GNSS-CORS device. The mobile phone demonstrates the widest range of elevation values, with intermediate elevation measurements, whereas Google Earth software presents the smallest range, yielding elevation values closely aligned with those obtained from the mobile phone.

3.2. Generation process results of DTM data from UAV Devices

In this study, the data acquired from UAVs were generated through a systematic process involving the transfer of photographic images captured by UAVs to a computer system. Once transferred, these images were subjected to detailed processing using the Pix4D photogrammetric software application. The processing workflow included tasks such as image alignment (Figure 8), point cloud generation, and orthophoto creation, which collectively contributed to the comprehensive analysis and interpretation of the UAV-collected data.

The data collected through the deployment of DJI Phantom 4 and Phantom 4 RTK UAVs in the context of this research were processed using Pix4D software. This process consisted in the creation and storage of DTM datasets. The elevation raster data, derived from these DTM datasets, were then analyzed and are visually represented in Figure 9. This figure illustrates the spatial distribution of elevation across the surveyed area, providing a detailed and comprehensive depiction of the terrain's topographical variations as obtained from the UAV-based measurements.

The DJI Phantom 4 exhibits the highest minimum elevation at 1140.18 meters and the highest maximum elevation at 1103.17 meters, thereby encompassing an elevation range of 37.01 meters (Figure 9). In contrast, the DJI Phantom 4 RTK device records the lowest minimum elevation at 1127.49 meters and the lowest maximum elevation at 1104.48 meters, resulting in an elevation range of 23.01 meters.

3.3. Comparison of DEM and DTM data

DEM and DTM data were generated utilizing data sourced from all relevant sources within the scope of this study. Consequently, the results of the computations conducted within the delineated study area are represented as elevations above sea level in the columns labeled elevation "Min", "Max", "Difference", and "Average" in Table 2.

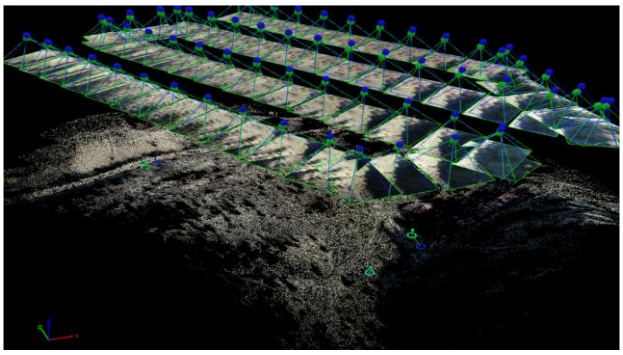

Figure 8. Image alignment from the study area

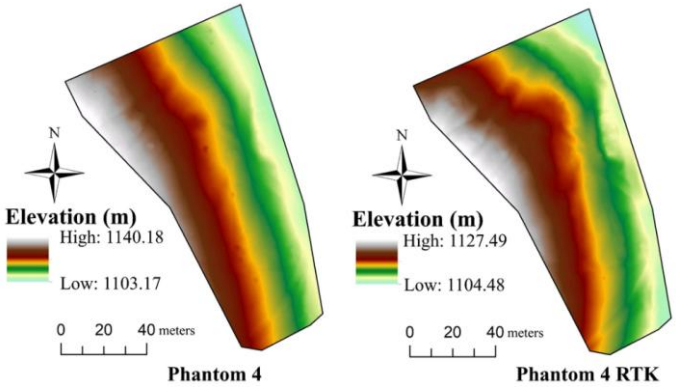

Figure 9. DTM data generated from DJI Phantom 4 and DJI Phantom 4 RTK

Table 2. Some statistics calculated for DEM and DTM data

	Elevation (m)			
	Min.	Max.	Difference	Average
GNSS-CORS	1104.74	1127.78	23.04	1115.14
GPS	1025.29	1048.35	23.06	1037.03
Mobile phone	1065.03	1094.83	29.8	1076.13
Google Earth	1068.26	1088.91	20.65	1079.36
Phantom 4	1103.17	1140.18	37.01	1120.02
Phantom 4 RTK	1104.48	1127.49	23.01	1115.14

In analyzing the measurement data acquired from the Phantom 4 RTK and Phantom 4 drones, GNSS-CORS, GPS devices, and mobile phones employed in this study, a comparative assessment with the Google Earth DEM data reveals notable discrepancies. This comparison, illustrated in Table 2, highlights variances in the lowest and highest elevation values, as well as in the average height measurements of the terrain. These discrepancies can be attributed to the inherent technological differences among the measurement instruments, despite their simultaneous operation. The diverse methodologies and technological frameworks underlying each device contribute to these variations.

As detailed in Table 2 and depicted in Figure 10, the ranking of "Elevation" differences from lowest to highest reveals that the DJI Phantom 4 RTK demonstrates a performance closely followed by the GNSS-CORS device, which presents a very similar value. However, it is noteworthy that the DJI Phantom 4 exhibits the highest elevation difference among all the devices evaluated. This ranking indicates that while the DJI Phantom 4 RTK and the GNSS-CORS device perform comparably, the DJI Phantom 4 distinctly exceeds the others in terms of elevation discrepancy, highlighting its relative positional deviation in the dataset. It was observed that the GPS device employed in this study exhibited inaccuracies in height measurement when compared to the GNSS-CORS device, which was utilized for control purposes. However, the GPS device was able to detect the variations in terrain heights with a degree of accuracy that was nearly equivalent to that of the GNSS-CORS device. The Google Earth dataset, created by combining elevation data from satellite measurements, works well for flat terrain but becomes less accurate when applied to sloped areas. While the satellite data provides a good overall view of the landscape, it doesn't always capture the finer details of the terrain, especially on slopes, which can lead to discrepancies between the virtual model and the actual topography (Hoffmann and Winde 2010). As a result, while Google Earth is a reliable tool for many uses, its effectiveness in representing complex, uneven surfaces is somewhat limited.

In this study, the calculation of latitude, longitude, and altitude values for identical locations across all generated land surfaces, random points were created utilizing the "Random Points" command within the ArcGIS software environment. The altitude values for these points were then computed based on the DEMs and DTMs that were produced as part of this research. Following the computation, the altitude values obtained from all DEM and DTM datasets were systematically consolidated into a comprehensive table. This consolidation enabled a detailed comparison of altitude values across different datasets. In this study, the discrepancies between the values obtained from the DEM and DTM datasets were systematically assessed. Following the identification of these discrepancies, their squared values were computed, allowing for the determination of the squared errors for each randomly selected point, as detailed below. The table of elevation values, which highlights the differences between the computed elevation values and the reference measurements GNSS-CORS, is presented in Appendix 1.

To ascertain the cumulative RMSE value, deviations from each DEM and DTM data set were collected (Figure 10). An analysis of Appendix 1 reveals that the Phantom 4 RTK device yields values closest to those of the GNSS-CORS device, with a deviation of merely 0.00001 meters. This is succeeded by the Phantom 4 with a deviation of 0.00336 meters, Google Earth with 0.12664 meters, mobile phones with 0.15230 meters, and, lastly, the GPS device, which exhibits the highest deviation of 0.61070 meters. Although all devices generally show the study area with the same accuracy in terms of latitude and longitude, it has been determined that there are serious differences in terms of elevation. These differences are thought to be of a type that will create serious calculation errors, especially in cut-fill volume calculation.

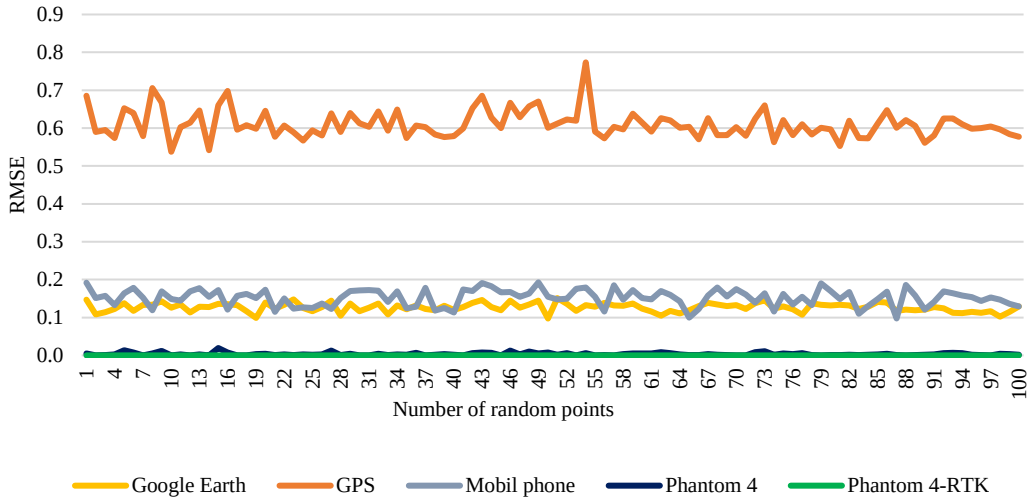

Figure 10. Comparison of RMSE values of random points

The RMSE value ranges from 0 to infinity, with its interpretative significance largely determined by its proximity to zero. The RMSE values recorded for the Phantom 4 RTK and Phantom 4 devices are 0.00001 meters and 0.00336 meters, respectively, highlighting the superior precision of the former. These results suggest that GNSS-CORS and UAV technologies are capable of capturing data with exceptional accuracy and are highly advantageous due to their relatively brief operational times. Conversely, for measurement studies where broader data sensitivity is acceptable, alternatives such as GPS, mobile phone, or Google Earth datasets may be preferred. In this regard, Table 3 provides a comprehensive summary of the measurement durations (in minutes) and costs (in US dollar) associated with the devices used in this study, conducted on a medium-sloped, one-hectare area.

Upon analysis of Table 3, it becomes evident that the Phantom 4 RTK, priced at $6500, offers the highest cost-to-measurement time efficiency, surpassing other devices. This is followed in descending order by the GNSS-CORS device at $4300, the Phantom 4 at $2700, a mobile phone at $2250, a GPS device at $30, and the alternative approach utilizing Google Earth datasets. Additionally, when considering the spatial resolution of the generated DEMs and DTMs, it is apparent that the GNSS-CORS and UAV devices generally exhibit superior performance compared to the other datasets. These results are consistent with the results from Seki (2017), Çetin (2019), and Bozkurt (2019), as well as the research conducted by Yılmaz et al. (2013), Özçelik and Buğday (2022), and Kinali and Çalişkan (2022).

Table 3. Measurement operation times and costs made with the devices used in the study

	Measuring period (minute/ha)	Spatial resolution (m*m)	Cost (USD)	Daily rental cost (USD)
Phantom 4 RTK	7	0.15x0.15	6500	60
Phantom 4	8	0.16x0.16	2700	40
GNSS-CORS	32	0.16x0.16	4300	30
GPS	17	0.77x0.77	30	10
Google Earth	20	0.76x0.76	Free	Free
Mobil phone	15	0.71x0.71	2250	Free

Investigations into the utilization of Unmanned Aerial Vehicles (UAVs) within the realms of photogrammetry and mapping consistently highlight the significant advantages these technologies offer in terms of both precision and cost-efficiency. Empirical evidence from various studies underscores the efficacy of UAVs in achieving high levels of accuracy in mapping applications. Similar to this study, research conducted by Akgul et al. (2018), Aykut (2019), and Akar et al. (2021) provides a comparative analysis of the accuracy metrics of UAVs, specifically evaluating their performance in the vertical plane against their remarkable precision in the horizontal plane. Their results indicate that UAVs can achieve exceptional accuracy levels in both dimensions. Similar to our study, further reinforcing these conclusions, Akgül et al. (2016), Türk and Öcalan (2020), Zhang et al. (2022), and Güngör et al. (2022) contribute additional evidence supporting the capability of UAVs to deliver high accuracy in photogrammetric applications. These studies collectively affirm that UAV technology is capable of producing highly accurate results, thereby enhancing the effectiveness and reliability of mapping practices. The convergence of these results across multiple research efforts highlights the robust potential of UAVs to revolutionize the field of photogrammetry through their precision and cost-effective benefits.

In this study, measurements were conducted over a 1-hectare area. The deviations along the horizontal axis were negligible and thus were disregarded within the scope of the study. Conversely, the vertical deviations exhibited considerable variation contingent upon the technology employed by the measurement devices. The error rates associated with UAV, GNSS-CORS, GPS, and mobile phone devices discussed herein are anticipated to escalate with an increase in area. To mitigate these deviations, it is crucial to incorporate the GNSS-CORS device in all measurement-related studies.

4. Conclusion

This study provides a comparative analysis of the measurement performances of various devices, each characterized by distinct technical specifications and

measurement sensitivities. In addition to evaluating these devices, which are extensively utilized and increasingly incorporated into contemporary measurement studies, the spatial sensitivity of each device has been considered as a criterion in the assessments. In this study, measurements were conducted on a one-hectare area with an average slope. Various measurement devices were employed, including UAV, GNSS-CORS, GPS, and mobile phones, each possessing distinct features. Additionally, elevation data for the same area was obtained using Google Earth software and subsequently transferred to a GIS environment. Based on the results of this study, it was established that the GNSS-CORS and RTK-enabled UAV demonstrated exceptional measurement precision. In contrast, the UAV operating without RTK capabilities exhibited standard measurement accuracy, while other devices delivered measurements with significantly lower precision. The results underscore the critical importance of utilizing RTK-enabled devices in applications demanding high precision, such as excavation and fill calculations, road construction assessments, and mass estimations. Conversely, for studies constrained by lower budgets and precision requirements, GPS, mobile phone data, and Google Earth can be considered viable alternatives for measurements that prioritize latitude and longitude accuracy over altitude precision.

When evaluating forested regions and their immediate environments, it is well-known that the requisite measurements are both complex and time-intensive compared to those in areas with gentler gradients. Given that the forested expanses in our country are predominantly situated in mountainous and inclined terrains, measurement activities essential for the ongoing management of forestry operations are typically characterized as challenging and protracted. The sensitivity of measurements and associated error rates are contingent upon the technological specifications of the devices employed, which can vary considerably based on the technology in use. Therefore, it is imperative to delineate the specific applications and optimal contexts for different devices, alongside assessing their efficiency and cost-effectiveness. Expanding the scope of this and similar research endeavors is anticipated to enhance clarity and precision regarding the suitability of various devices or datasets for specific measurement objectives.

Future research should involve a comprehensive reassessment of time-cost values, taking into account the prevailing temporal conditions and the advancements in rapidly evolving technologies, as well as the emergence of novel computer algorithms pertinent to land surveying and data set generation. Such studies are inherently subject to iterative refinement and enhancement. Moreover, augmenting the workforce engaged in engineering surveying, particularly those proficient in utilizing accessible technologies, is crucial for ensuring data reliability and fostering a more informed decision-making process.

Acknowledgement

This research, titled "*Calculation of Digital Land Surface Using Different Measuring Devices in Forestry and Comparison of Device Performances (Çerkeş Sample)*" by Ali KARACA, was carried out in the Department of Forest Engineering, Graduate School of Natural and Applied Sciences at Çankırı Karatekin University, is derived from master's thesis completed in 2023.

Appendix

Appendix 1. The differences between the computed elevation values and the reference measurements

Line No	Google Earth	GPS	Mobil	P4	P4RTK	Line No	Google Earth	GPS	Mobil	P4	P4RTK
1	0.14678	0.68550	0.19146	0.00535	0.00001	51	0.15121	0.61192	0.14810	0.00162	0.00000
2	0.10854	0.58976	0.15101	0.00000	0.00012	52	0.13602	0.62247	0.14980	0.00573	0.00003
3	0.11414	0.59521	0.15697	0.00105	0.00001	53	0.11721	0.61969	0.17610	0.00007	0.00000
4	0.12218	0.57401	0.13283	0.00278	0.00000	54	0.13281	0.77355	0.17886	0.00582	0.00000
5	0.13769	0.65252	0.16376	0.01340	0.00001	55	0.12844	0.59094	0.15466	0.00015	0.00000
6	0.11702	0.63945	0.17823	0.00788	0.00001	56	0.13845	0.57260	0.11553	0.00049	0.00000
7	0.13381	0.57893	0.15202	0.00001	0.00001	57	0.13183	0.60301	0.18479	0.00017	0.00001
8	0.13351	0.70595	0.11920	0.00507	0.00000	58	0.13091	0.59688	0.14740	0.00322	0.00000
9	0.14244	0.66758	0.16899	0.01199	0.00002	59	0.13690	0.63775	0.17209	0.00487	0.00000
10	0.12552	0.53758	0.14843	0.00000	0.00000	60	0.12306	0.61449	0.15155	0.00460	0.00001
11	0.13457	0.60249	0.14440	0.00217	0.00000	61	0.11583	0.59037	0.14761	0.00497	0.00002
12	0.11303	0.61445	0.16918	0.00007	0.00001	62	0.10489	0.62637	0.16941	0.00822	0.00001
13	0.12880	0.64611	0.17701	0.00284	0.00000	63	0.11764	0.62060	0.15981	0.00562	0.00001
14	0.12717	0.54142	0.15445	0.00013	0.00000	64	0.11095	0.60114	0.14285	0.00283	0.00002
15	0.13563	0.66021	0.17277	0.01937	0.00001	65	0.11901	0.60360	0.09988	0.00052	0.00001
16	0.13478	0.69814	0.12048	0.00736	0.00000	66	0.12978	0.57022	0.12224	0.00080	0.00000
17	0.13249	0.59587	0.15677	0.00002	0.00000	67	0.13828	0.62603	0.15817	0.00361	0.00000
18	0.11623	0.60779	0.16226	0.00024	0.00001	68	0.13451	0.58112	0.17882	0.00143	0.00000
19	0.09902	0.59816	0.15104	0.00294	0.00004	69	0.12978	0.58167	0.15560	0.00068	0.00000
20	0.13943	0.64536	0.17338	0.00440	0.00000	70	0.13240	0.60264	0.17454	0.00001	0.00000
21	0.12354	0.57699	0.11493	0.00086	0.00002	71	0.12218	0.57947	0.16030	0.00012	0.00001
22	0.13353	0.60716	0.15029	0.00263	0.00000	72	0.13798	0.62487	0.13922	0.00839	0.00002
23	0.14779	0.58933	0.12351	0.00080	0.00000	73	0.14537	0.65983	0.16415	0.01129	0.00000
24	0.12534	0.56750	0.12696	0.00213	0.00013	74	0.12294	0.56291	0.11557	0.00130	0.00000
25	0.11669	0.59411	0.12466	0.00160	0.00000	75	0.12961	0.62088	0.16257	0.00460	0.00000
26	0.12734	0.58091	0.13647	0.00259	0.00001	76	0.12174	0.58135	0.13416	0.00322	0.00002
27	0.14461	0.63896	0.12266	0.01302	0.00004	77	0.10727	0.60994	0.15471	0.00576	0.00004
28	0.10434	0.58986	0.15151	0.00115	0.00000	78	0.13805	0.58293	0.13223	0.00105	0.00001
29	0.13722	0.63991	0.16954	0.00396	0.00000	79	0.13331	0.60095	0.19014	0.00009	0.00001
30	0.11688	0.61257	0.17146	0.00000	0.00001	80	0.13220	0.59685	0.16999	0.00098	0.00000
31	0.12623	0.60327	0.17214	0.00001	0.00013	81	0.13307	0.55264	0.14860	0.00041	0.00000
32	0.13661	0.64364	0.17086	0.00431	0.00000	82	0.13204	0.61980	0.16741	0.00146	0.00000
33	0.10803	0.59287	0.14120	0.00099	0.00001	83	0.12209	0.57343	0.11011	0.00068	0.00000
34	0.13141	0.64934	0.16921	0.00242	0.00001	84	0.12880	0.57269	0.13034	0.00128	0.00000
35	0.12190	0.57360	0.12396	0.00193	0.00000	85	0.14127	0.61194	0.14839	0.00257	0.00000
36	0.13150	0.60704	0.12821	0.00649	0.00001	86	0.13949	0.64702	0.16775	0.00377	0.00002
37	0.12248	0.60254	0.17802	0.00007	0.00000	87	0.11764	0.60079	0.09739	0.00046	0.00001
38	0.11884	0.58321	0.11811	0.00164	0.00002	88	0.12043	0.62141	0.18598	0.00011	0.00000
39	0.13076	0.57608	0.12479	0.00346	0.00001	89	0.11871	0.60593	0.15758	0.00058	0.00002
40	0.12024	0.57870	0.11327	0.00123	0.00001	90	0.12115	0.56143	0.12047	0.00200	0.00000
41	0.12734	0.59946	0.17365	0.00001	0.00017	91	0.12715	0.58033	0.14074	0.00287	0.00000
42	0.13829	0.65286	0.16962	0.00583	0.00001	92	0.12420	0.62579	0.16907	0.00612	0.00000
43	0.14602	0.68556	0.19085	0.00755	0.00002	93	0.11261	0.62538	0.16395	0.00704	0.00001
44	0.12716	0.62753	0.18225	0.00688	0.00000	94	0.11162	0.61040	0.15779	0.00589	0.00001
45	0.11889	0.59987	0.16665	0.00034	0.00000	95	0.11521	0.59831	0.15352	0.00122	0.00003
46	0.14405	0.66690	0.16692	0.01265	0.00000	96	0.11264	0.59970	0.14320	0.00060	0.00002
47	0.12624	0.62906	0.15442	0.00264	0.00000	97	0.11621	0.60447	0.15320	0.00022	0.00000
48	0.13448	0.65716	0.16343	0.00994	0.00000	98	0.10226	0.59641	0.14731	0.00447	0.00002
49	0.14475	0.66988	0.19271	0.00520	0.00001	99	0.11493	0.58426	0.13612	0.00306	0.00001
50	0.09722	0.60094	0.15451	0.00742	0.00003	100	0.12888	0.57706	0.12900	0.00196	0.00000

References

Akar, A., Akar, Ö., Bayata, H. F., 2021. SenseFly eBeeX İHA ile üretilen ortofotonun konum doğruluğunun incelenmesi. Türkiye İnsansız Hava Araçları Dergisi, 3(2): 65–68.

Akgul, M., Yurtseven, H., Gulci, S., Akay, A. E., 2018. Evaluation of UAV- and GNSS-Based DEMs for Earthwork Volume. Arabian Journal for Science and Engineering, 43(4): 1893–1909.

Akgül, M., Yurtseven, H., Demir, M., Akay, A. E., Gülci, S., Öztürk, T., 2016. İnsansız hava araçları ile yüksek hassasiyette sayısal yükseklik modeli üretimi ve ormancılıkta kullanım olanakları. İstanbul Üniversitesi Orman Fakültesi Dergisi, 66(1):104-118.

Apple, 2024. Apple Iphone 13 Pro Mobil Phone. Specifications of Iphone 13 Pro. https://support.apple.com/en-us/111871, Erişim: 15.01.2023.

Aykut, N.O., 2019. İnsansız Hava Araçlarının kıyı çizgisinin belirlenmesinde kullanılabilirliğinin araştırılması. Geomatik, 4(2): 141–146.

Boukoberine, M. N., Zhou, Z., Benbouzid, M., 2019. A critical review on unmanned aerial vehicles power supply and energy management: Solutions, strategies, and prospects. Applied Energy, 255: 113823.

Bozkurt, N., 2019. İnsansız hava araçlarında (İHA) düşük maliyetli GNSS alıcılarının konum belirleme performansı. Yüksek lisans tezi, Gebze Teknik Üniversitesi, Fen Bilimleri Enstitüsü, Gebze.

Buğday, E., 2018. Capabilities of using UAVs in Forest Road Construction Activities. European Journal of Forest Engineering, 4(2): 56–62.

Buğday, E., 2019. Orman yönetiminde insansız hava aracı uygulamaları. Orman yönetiminde insansız hava aracı uygulamaları. 2nd International Eurasian Conference on Biological and Chemical Sciences (EurasianBioChem 2019), 28-29 June 2019, Ankara, Türkiye, pp. 1617–1621.

Bülbül, S., İnal, C., Yildirim, Ö., 2015. Comparison of RTK, network RTK and total station data in determination of point positions. Harita Teknolojileri Elektronik Dergisi. 7(2): 27-35.

CHC, 2024. CHC-X91 GNSS-CORS. CHC Navigation. https://chcnav.es/es/productos/x91-gnss/chc-Manual-Gps-Centimetrico-X91-en.pdf, Erişim: 15.01.2023.

Çetin, O., 2019. Hava fotoğrafları ve insansız hava aracı görüntülerinden arazi topoğrafyası ölçümü, sonuçların analizi ve karşılaştırması (Haymana Yeşilyurt köyü uygulaması) Yüksek lisans tezi, Konya Teknik Üniversitesi, Lisansüstü Eğitim Enstitüsü, Konya.

DJI, 2024a. DJI Phantom 4. Support for Phantom 4. https://www.dji.com/support/product/phantom-4, Erişim: 15.01.2023.

DJI, 2024b. DJI Phantom 4 RTK. Support for Phantom 4 RTK Enterprise. https://enterprise.dji.com/phantom-4-rtk/specs, Erişim: 15.01.2023.

Durgun, H., Çoban, H.O., Eker, M., 2022. İnsansız hava aracıyla elde edilen hava fotoğraflarından kızılçam ağaçlarının çap ve boylarının ölçümü ve gövde hacminin tahmini. Turkish Journal of Forestry, 23(4):255–267.

Durgun, H., Yılmaz İnce, E., İnce, M., Çoban, H.O., Eker, M., 2023. Evaluation of tree diameter and height measurements in UAV data by integrating Remote Sensing and Machine Learning Methods. Gazi Journal of Engineering Sciences, 9(4): 113–125.

Eryılmaz, E., 2019. Karayolu projelerinde bilgisayar programları kullanılarak proje aşamalarının mühendislik açısından değerlendirilmesi. Yüksek lisans tezi, İskenderun Teknik Üniversitesi, Mühendislik ve Fen Bilimleri Enstitüsü, Hatay.

ESRI, 2022. Random Points. https://desktop.arcgis.com/en/arcmap/latest/tools/spatial-analyst-toolbox/idw.htm, Erişim: 03.03.2023.

ESRI, 2023. IDW (Inverse Distance Weighting). https://desktop.arcgis.com/en/arcmap/latest/tools/spatial-analyst-toolbox/idw.htm, Erişim: 03.03.2023.

Famiglietti, N. A., Cecere, G., Grasso, C., Memmolo, A., Vicari, A., 2021. A Test on the Potential of a low cost unmanned aerial vehicle RTK/PPK solution for precision positioning. Sensors, 21(11): 3882.

Fascista, A., 2022. Toward integrated large-scale environmental monitoring using WSN/UAV/Crowdsensing: A Review of applications, signal processing, and future perspectives. Sensors, 22(5): 1824.

Garmin, 2024. Garmin Oregon 550 GPS. Garmin Oregon 550 GPS. https://www.garmin.com/en-US/p/26875, Erişim: 15.01.2023.

Grindley, B., Phillips, K., Parnell, K. J., Cherrett, T., Scanlan, J., Plant, K. L., 2024. Over a decade of UAV incidents: A human factors analysis of causal factors. Applied Ergonomics, 121: 104355.

Gupta, A., Afrin, T., Scully, E., Yodo, N., 2021. Advances of UAVs toward Future Transportation: The State-of-the-Art, Challenges, and Opportunities. Future Transportation, 1(2): 326–350.

Güngör, R., Uzar, M., Atak, B., Yilmaz, O. S., Gümüş, E., 2022. Orthophoto production and accuracy analysis with UAV photogrammetry. Mersin Photogrammetry Journal, 4(1): 1–6.

Fan, S., Bose, N., Liang, Z., 2024. Polar AUV Challenges and Applications: A Review. Drones, 8(8): 413.

Hoffmann, E., Winde, F., 2010. Generating high-resolution digital elevation models for wetland research using Google EarthTM imagery: an example from South Africa. Water SA, 36(1): 53-68.

Huggins, R. A., Giersch, G. E. W., Belval, L. N., Benjamin, C. L., Curtis, R. M., Sekiguchi, Y., Peltonen, J., Casa, D. J., 2020. The validity and reliability of global positioning system units for measuring distance and velocity during linear and team sport simulated movements. Journal of Strength and Conditioning Research 34(11):3070-3077.

Julge, K., Ellmann, A., Köök, R., 2019. Unmanned aerial vehicle surveying for monitoring road construction earthworks. The Baltic Journal of Road and Bridge Engineering, 14(1): 1–17.

Kahveci, M., 2009. Gerçek zamanlı ulusal sabit GNSS CORS Ağları ve düşündürdükleri. Jeodezi ve Jeoinformasyon Dergisi, 100: 13–20.

Karaali, C., Yıldırım, Ö., 1996. Global konum belirleme sistemi (GPS). Pamukkale Üniversitesi Mühendislik Bilimleri Dergisi, 2(2): 103–108.

Karagöz, S. D., Kincal, C., Koca, M.Y., 2020. Menderes Masifi'nde Açılmış açık ocak albit madenindeki bir duraysızlığın nedenlerinin araştırılması ve robotic total station cihazı kullanılarak yenilme öncesinde şev hareketlerinin izlenmesi. Jeoloji Mühendisliği Dergisi, 44(1): 41–66.

Kinali, M., Çalişkan, E., 2022. Use of unmanned aerial vehicles in forest road projects. Bartın Orman Fakültesi Dergisi, 24(3):530–541.

Martinez, J.G., Gheisari, M., Alarcón, L.F., 2020. UAV integration in Current construction safety planning and monitoring processes: Case study of a high-rise building construction project in Chile. Journal of Management in Engineering, 36(3), 05020005.

Özçelik, A., Buğday, E., 2022. Generating Landslide susceptibility maps using mathematical models and UAV data: The Case of Çankırı region in Türkiye. European Journal of Forest Engineering, 8(1): 1–10.

Park, H. C., Rachmawati, T.S.N., Kim, S., 2022. UAV-Based high-rise Buildings earthwork monitoring—A case study. Sustainability, 14(16):10179.

Putra, A. B., Arumsari, P., Cahyono, C., Sarigih, J.F.B., Kosalim, V., 2023. Building infrastructure analysis using total station and unmanned aerial vehicle drone for surveying and modelling. Proceedings of the 6th International Conference on Eco Engineering Development 2022 16-17 September 2022 (published online 2 May 2023), Jakarta, Indonesia, pp. 1-8.

Ren, H., Zhao, Y., Xiao, W., Hu, Z., 2019. A review of UAV monitoring in mining areas: Current status and future perspectives. International Journal of Coal Science and Technology, 6(3): 320–333.

Robakowska, M., Ślęzak, D., Żuratyński, P., Tyrańska-Fobke, A., Robakowski, P., Prędkiewicz, P., Zorena, K., 2022. Possibilities of using UAVs in pre-hospital security for medical emergencies. International Journal of Environmental Research and Public Health, 19(17): 10754.

Schiefer, F., Kattenborn, T., Frick, A., Frey, J., Schall, P., Koch, B., Schmidtlein, S., 2020. Mapping forest tree species in high resolution UAV-based RGB-imagery by means of convolutional neural networks. ISPRS Journal of Photogrammetry and Remote Sensing, 170: 205–215.

Seki, M., 2017. İnsansız hava araçlarının hacim hesaplarında kullanılabilirliği. Yüksek lisans tezi. Afyon Kocatepe Üniversitesi, Fen Bilimleri Enstitüsü, Afyonkarahisar.

Śledź, S., Ewertowski, M.W., Piekarczyk, J., 2021. Applications of unmanned aerial vehicle (UAV) surveys and Structure from Motion photogrammetry in glacial and periglacial geomorphology. Geomorphology, 378: 107620.

Şanlıyüksel Yücel, D., Yücel, M.A., 2017. Terk edilmiş kömür ocaklarında oluşan maden göllerinin hidrokimyasal özelliklerinin belirlenmesi ve insansız hava aracı ile üç boyutlu modellenmesi. Pamukkale Üniversitesi Mühendislik Bilimleri Dergisi, 23(6): 780–791.

Tercan, E., 2017. Karayolu projelerinde insansız hava aracı ile üretilen sayısal arazi modelinin değerlendirilmesi: Bucak-Kocaaliler yolu örneği. Mehmet Akif Ersoy Üniversitesi Fen Bilimleri Enstitüsü Dergisi, 8(2): 172–183.

Türk, T., Öcalan, T., 2020. PPK GNSS Sistemine sahip insansız hava araçları ile elde edilen fotogrametrik ürünlerin doğruluğunun farklı yaklaşımlarla irdelenmesi. Türkiye Fotogrametri Dergisi, 2(1): 22–28.

Yılmaz, V., Akar, A., Akar, Ö., Güngör, O., Karslı, F., Gökalp, E., 2013. İnsansız hava aracı ile üretilen ortofoto haritalarda doğruluk analizi. TUFUAB 2013 Türkiye Ulusal Fotogrametri ve Uzaktan Algılama Birliği VII. Teknik Sempozyumu, 23-25 May, Trabzon, Turkey, pp. 1-6.

Zhang, B., Li, X., Du, H., Zhou, G., Mao, F., Huang, Z., Zhou, L., Xuan, J., Gong, Y., Chen, C., 2022. Estimation of urban forest characteristic parameters using UAV-Lidar coupled with canopy volume. Remote Sensing, 14(24): 6375.

.